Since January 2020 Elsevier has created a COVID-19 resource centre with free information in English and Mandarin on the novel coronavirus COVID-19. The COVID-19 resource centre is hosted on Elsevier Connect, the company's public news and information website.

Virology 409 (2011) 121–131

Contents lists available at ScienceDirect

Virology

journal homepage: www.elsevier.com/locate/yviro

Deficient incorporation of spike protein into virions contributes to the lack of infectivity following establishment of a persistent, non-productive infection in oligodendroglial cell culture by murine coronavirus

Yin Liu [a], Werner Herbst [b], Jianzhong Cao [a], Xuming Zhang [a,*]

[a] Department of Microbiology and Immunology, University of Arkansas for Medical Sciences, Little Rock, AR 72205-7199, USA
[b] Institut für Hygiene und Infektionskrankheiten der Tiere, Justus-Liebig-Universität Giessen, Giessen, Germany

ARTICLE INFO

Article history:
Received 1 September 2010
Returned to author for revision
18 September 2010
Accepted 3 October 2010
Available online 28 October 2010

Keywords:
Coronavirus
Oligodendrocyte
Persistence

ABSTRACT

Infection of mouse oligodendrocytes with a recombinant mouse hepatitis virus (MHV) expressing a green fluorescence protein facilitated specific selection of virus-infected cells and subsequent establishment of persistence. Interestingly, while viral genomic RNAs persisted in infected cells over 14 subsequent passages with concomitant synthesis of viral subgenomic mRNAs and structural proteins, no infectious virus was isolated beyond passage 2. Further biochemical and electron microscopic analyses revealed that virions, while assembled, contained little spike in the envelope, indicating that lack of infectivity during persistence was likely due to deficiency in spike incorporation. This type of non-lytic, non-productive persistence in oligodendrocytes is unique among animal viruses and resembles MHV persistence previously observed in the mouse central nervous system. Thus, establishment of such a culture system that can recapitulate the in vivo phenomenon will provide a powerful approach for elucidating the mechanisms of coronavirus persistence in glial cells at the cellular and molecular levels.

Introduction

Murine coronavirus mouse hepatitis virus (MHV) is a member of the *Coronaviridae*. It is an enveloped, positive-strand RNA virus. The viral envelope contains three or four structural proteins, depending on viral strains (Lai and Cavanagh, 1997). The spike (S) protein is a glycoprotein with a molecular weight of approximately 180 kilo Dalton (kDa). For some MHV strains such as JHM and A59, the S protein can be cleaved by a furin-like proteinase into two subunits: the amino terminal S1 and the carboxyl-terminal S2. The S1 subunit is thought to form the globular head of the spike and is responsible for the initial attachment of the virus to the receptor on cell surface. The S2 subunit, which forms the stalk portion of the spike and which anchors the S protein to the viral envelope, facilitates the fusion between viral envelope and cell membrane and cell–cell fusion (Chambers et al., 1990; de Groot et al., 1987; de Haan et al., 2004; Gallagher et al., 1991; Kubo et al., 1994; Luytjes et al., 1987; Nash and Buchmeier, 1997; Stauber et al., 1993; Suzuki and Taguchi, 1996; Zhu et al., 2009). It is therefore an important determinant for viral infectivity, pathogenicity and virulence (Boyle et al., 1987; Collins et al., 1982; Phillips et al., 1999). The small envelope (E) protein and the membrane (M) protein play a key role in virus assembly (Vennema et al., 1996; Yu et al., 1994). The nucleocapsid (N) protein is a phosphoprotein of approximately 50 kDa and is associated with the RNA genome to form the nucleocapsid inside the envelope (Lai and Cavanagh, 1997; Stohlman and Lai, 1979). Upon entry into host cells, the viral genomic RNA serves as an mRNA for translation of the viral polymerase polyprotein from the 5′ most overlapping open reading frames 1a and 1b (Lai and Cavanagh, 1997). The polyprotein is then processed into 16 nonstructural proteins (nsp's), which possibly along with host factors form replication and transcription complexes that generate a nested-set of subgenomic mRNAs (Lai and Cavanagh, 1997; Snijder et al., 2003). Each subgenomic mRNA is translated into a structural or nonstructural protein. The structural proteins are assembled into virions in cytoplasmic vesicles (Vennema et al., 1996), which are then released (exocytosed) from the infected cell.

MHV can infect rodents, causing hepatitis, enteritis, and central nervous system (CNS) diseases. In the CNS, acute encephalitis usually occurs during the first week of infection, and acute demyelination can be detected histologically as early as 6 days post infection (p.i.). By the end of the second week, if the mice survive virus infection, most of the viruses are cleared from the CNS, and demyelination develops. Although infectious virus can no longer be isolated from the CNS during the chronic phase (≈3 weeks p.i.), viral RNAs are continuously detectable by Northern blot or reverse transcription-polymerase chain reaction (RT-PCR). Demyelination continues to peak at around 30 days p.i., and then slowly decreases until over a year p.i.,

* Corresponding author. Department of Microbiology and Immunology, University of Arkansas for Medical Sciences, 4301 W. Markham Street, Slot 511, Little Rock, AR 72205, USA. Fax: +1 501 686 5359.
E-mail address: zhangxuming@uams.edu (X. Zhang).

0042-6822/$ – see front matter © 2010 Elsevier Inc. All rights reserved.
doi:10.1016/j.virol.2010.10.006

concomitant with viral RNA persistence (Bergmann et al., 2006; Das Sarma et al., 2000; Fleming et al., 1993a; Knobler et al., 1981, 1982; Lavi et al., 1984). Although the mechanisms of MHV-caused CNS demyelination are not known, it is believed that the host immune response plays an important role in the demyelination process (Dandeker and Perlman, 2002; Fleming et al., 1993b; Lai and Cavanagh, 1997; Lane et al., 2000; Matthews et al., 2002; Sorensen et al., 1987; Wang et al., 1990; Wu and Perlman, 1999, Wu et al., 2000). It has been shown that the development of demyelination in mice is associated with viral RNA persistence (Das Sarma et al., 2000; Knobler et al., 1982), but the mechanism of CNS persistence remains largely unknown.

Previously, a number of laboratories have attempted to establish an in vitro cell culture system for MHV persistence (Chen and Baric, 1996; Lavi et al., 1987; Sawicki et al., 1995; Schickli et al., 1997). While these studies have led to the establishment of MHV persistence in fibroblast 17Cl-1 cells, astrocytoma DBT cells and primary oligodendrocytes, infectious viruses continued to be produced, albeit at an extremely low level (Chen and Baric, 1996; Lavi et al., 1987; Sawicki et al., 1995; Schickli et al., 1997). Thus, such persistence does not resemble the phenomenon observed in mouse CNS. Although we have previously reported the establishment of a persistent, non-productive infection in a rat progenitor oligodendrocyte cell line (Liu et al., 2003; Liu and Zhang, 2005), the cells that harbor persistent viruses have not been confirmed, largely due to difficulty in separating infected cells from uninfected cells in a mixed culture. In an effort to establish a robust in vitro system that can faithfully recapitulate the in vivo phenomenon, in the current study we made several modifications in our experimental approach. We used a recombinant MHV that expresses a green fluorescence protein (GFP) such that infected cells can be easily identified and separated from non-infected cells. Using this approach, we were able to identify a new type of mouse oligodendroglial cell line (N20.1) that was persistently infected with MHV. Consistent with the results in rat progenitor oligodendrocytes (Liu and Zhang, 2005), viral RNA persisted for over 14 passages without the production of infectious virus. Significantly and unexpectedly, we discovered that persistently infected oligodendrocytes continued to produce viral particles but that these particles were deficient in incorporation of spike proteins on the virion surface, thus providing a mechanism for the lack of viral infectivity. To our knowledge, this is the first report in virology describing non-productive, persistent infection that continuously produces virus particles without infectivity due to a lack of spike protein incorporation.

Results

Establishment of persistent MHV infection in mouse oligodendroglial cells

We previously reported the establishment of a persistent MHV infection in a rat progenitor oligodendrocytic cell line CG-4 cells (Liu and Zhang, 2005). However, it was not clear in that study whether all cells or only a fraction of the cell population were initially infected with MHV. This question is important because the mechanism of persistence could be different under these conditions. To unequivocally address this question and to identify additional cell lines for such studies, we used the recombinant MHV-A59/GFP, which expresses the GFP, and two additional mouse oligodendrocytic cell lines N20.1 (Verity et al., 1993) and Oligo-neu (Jung et al., 1995). The rationale for using MHV-A59/GFP was to quantitatively assess the susceptibility of the cell population to virus infection and to track the extent of viral persistence following continuous passage of the cells. Thus, CG-4, N20.1 and Oligo-neu cells were infected with MHV-A59/GFP at an m.o.i. of 10, and were observed for GFP expression. We found that less than 0.1% of the CG-4 cells expressed strong GFP at 24 and 48 h p.i. (data not shown) while approximately 25% of N20.1 cells (Fig. 1B, a–b) and <20% of Oligo-neu cells exhibited strong fluorescence for the same time period (data not shown). Because of the highest cell number of GFP expression and relative ease in culture, N20.1 cells were used in all subsequent experiments described in this report.

Infected N20.1 cells were subjected to flow cytometric sorting (Fig. 1). Strong GFP-expressing cells were separated from non-GFP-expressing cells and were re-seeded into dishes (Fig. 1B, c–d), which were designated as VP1 (for passage 1 of virus-infected cells). To our surprise and disappointment, most of the green fluorescence disappeared by days 7 to 10 after seeding (Fig. 1B, e–f). Nevertheless, we continued to replenish the medium every other day and allowed the cells to grow to monolayers for additional 15 to 20 days. The monolayer cells were further passaged approximately every 8 days and were designated as VP2, VP3, and so forth.

To determine whether the infection was aborted after disappearance of the green fluorescence at the end of VP1, monolayer cells (approximately by 30 days after seeding of GFP-positive cells) were collected and the presence of viral genomic RNAs in the cells was determined by RT-PCR using 5 pairs of primers that represent 5 regions throughout the viral genome (Fig. 2A). Indeed, viral genomic RNAs were detected with all 5 pairs of primers (Fig. 2B), confirming the presence of the viral genome. We then isolated intracellular RNAs from various passages of the infected cells (VP1 to VP14) and used RNAs from acutely infected (VP0) and mock-infected N20.1 cells as a positive and negative control, respectively, for RT-PCR with the primer pair 5′N and 3′N. Results showed that viral genomic RNAs were present in all passages tested (Fig. 2C). Thus, real-time qRT-PCR (using primer pair 5′qPCR and 3′qPCR) was used to further quantify the viral genomic RNAs in these passages. It was found that in general the amount of viral genome decreased drastically from VP0 to VP4, but relatively slowly thereafter (Fig. 2D). These data demonstrate that viral genomic RNAs established persistence in N20.1 cells for a period of time long after the disappearance of GFP expression.

Loss of GFP expression is associated with aberrant transcription of subgenomic mRNA4 coding for GFP in persistently infected oligodendrocytes

Since viral genomic RNAs persisted (Fig. 2), we assumed that viral genomic replication must have taken place continuously, and so must have been the expression of the viral polymerase polyprotein, the ORF 1a/1b product. However, the eventual disappearance of GFP-positivity led us to further examine potential defects in viral gene expression in persistently infected N20.1 cells since the GFP ORF is under the control of the consensus intergenic sequence for subgenomic mRNA 4 (Fig. 3A) (Das Sarma et al., 2002). Thus, both the genomic regions encompassing the GFP coding sequence and the subgenomic mRNA4 at VP4 were specifically amplified by RT-PCR using the pair of primers 5′IG4–3′G5a and 5′Leader–3′G5a, respectively, and the PCR products were sequenced directly or following shotgun cloning. Interestingly, we found that the entire GFP ORF was intact within the persistent viral genome (data not shown) but that there were multiple species of subgenomic mRNA4 varying in size (Fig. 3B). These mRNAs contained a leader RNA fused at multiple sites downstream of the AUG translation initiation codon, thus effectively abolishing the expression of the GFP gene, a phenomenon reminiscent of the aberrant transcription described previously for MHV (Fischer et al., 1997; Zhang and Lai, 1994).

Expression of viral genes in persistently infected oligodendrocytes

The finding of aberrant transcription of subgenomic mRNA4 (GFP) led us to further examine whether the other viral subgenomic mRNAs were also transcribed aberrantly. Thus, the expression of viral subgenomic mRNAs coding for structural proteins and their protein products was assessed in various passages of the persistently infected N20.1 cells. As an example shown in Fig. 4, mRNA7 (for N gene) and mRNA3 (for S gene) were detected in various passages of the persistently infected cells but not

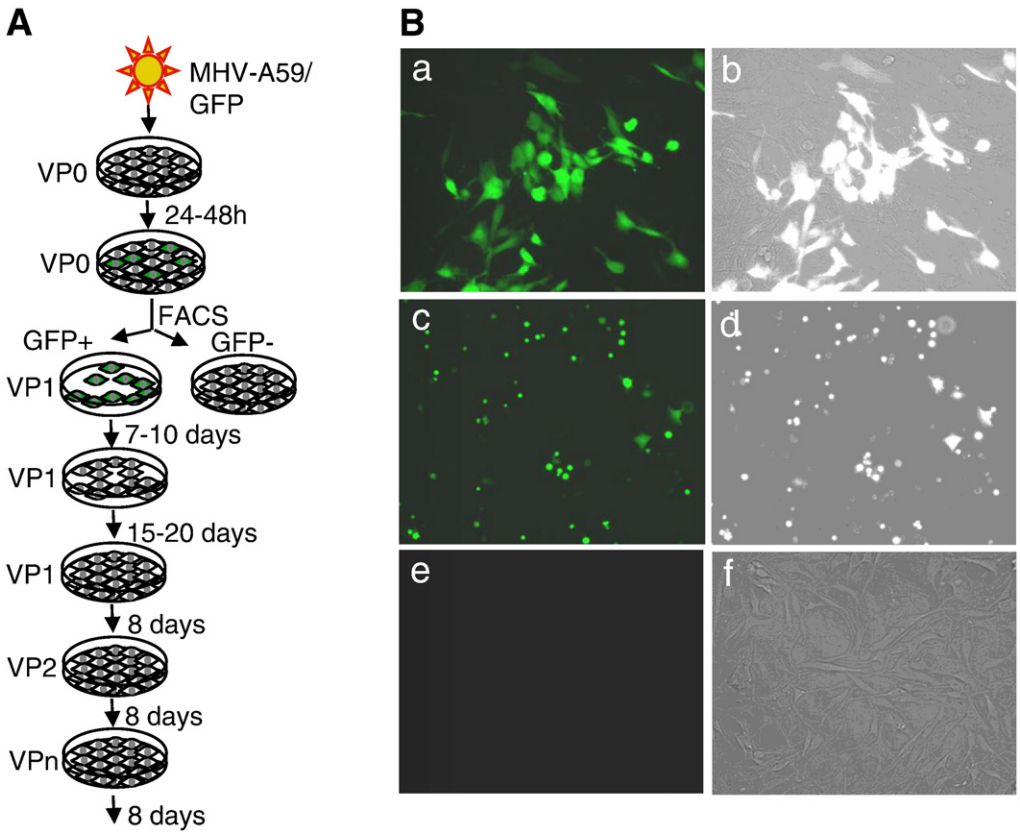

Fig. 1. Establishment of persistent MHV infection in oligodendroglial N20.1 cells. (A) Schematic diagram showing the procedure for establishing persistent infection. N20.1 cells were infected with MHV-A59/GFP at the m.o.i. of 10. Virus-infected cells at passage 0 (VP0) were subjected to FACS sorting. GFP-positive cells were re-seeded as VP1 and were allowed to grow to monolayer. VP1 cells were subsequently passaged, which are designated VP2, VP3, and so forth (VPn). (B) Monitoring GFP expression in virus-infected N20.1 cells. a, c, and e, showing GFP expression at various steps during the procedure; b, d, and f, showing the number of GFP-positive cells relative to the GFP-negative cells within the same field. The photographs were taken when both visible and fluorescent lights were turned on. a–b, GFP expression in VP0 cells at 48 h p.i. In general, approximately 25% of the cells were GFP-positive at 48 h p.i. c–d, GFP-positive cells following FACS sorting (VP1 cells), showing that almost all cells were GFP-positive. e–f, GFP-positive cells disappeared at subsequent passages of infected cells.

in mock-infected cells (Figs. 4B and C) by RT-PCR using a pair of primers (5′Leader–3′S1 and 5′Leader–3′N) that specifically detect the respective mRNA species (Fig. 4A). Similarly, viral N and S proteins were detected in these persistently infected cells by Western blot analysis and their expression appeared to decline over continuous passages when compared to the β-actin control (Figs. 4D and E). mRNAs for other structural proteins (M and E) were also detected (data not shown). These results confirm that virus-specific genes, especially structural genes, were expressed in persistently infected N20.1 cells.

Absence of infectious virus following establishment of genome persistence

To determine whether and to what extent infectious virus was produced during persistence, both culture medium and cell lysate were used for determining the presence of infectious virus in various passages by plaque assay. Indeed, virus titers were decreased from approximately 10^5 PFU/ml during acute infection (VP0) to about 10^2 PFU/ml at VP1. No infectious virus was detected beyond passage 2 (VP2) (Fig. 5A and further data not shown). To further determine the time point at which infectious virus was no longer recoverable, medium and cell lysate were collected at various days after seeding of the fluorescence-positive cells at VP1. The results showed that virus titer decreased gradually and reached to an undetectable level (the detection limit of the plaque assay was approximately 5 PFU/ml) by day 15 (Fig. 5B). These results, combined with the data shown in Figs. 1–4, reaffirm that MHV established persistence of viral genome in oligodendrocytes without the production of infectious viruses or with extremely low level of infectious virus (below the detection limit). This phenomenon resembles viral RNA persistence in the CNS of MHV-infected mice.

Biophysical and biochemical characterization of virions produced from persistently infected oligodendrocytes

Since no infectivity was detected in the medium and lysate of persistently infected N20.1 cells, we wondered whether viral particles had ever been made. Culture medium was collected from persistently infected N20.1 cells between passages 6 and 10. Virions, if any, were concentrated through 30% sucrose cushion and were further purified via 20–70% sucrose gradient by ultracentrifugation. The gradient was then fractionated and the buoyant density of each fraction was determined. Presence of viral N protein was determined by Western blot using an N-specific mAb. As shown in Fig. 6A, N protein was detected in the fractions 5 to 10, which correspond to the buoyant density between 1.14 and 1.20 g/ml. The standard buoyant density in sucrose for MHV-A59 is 1.18–1.19 g/ml (Liebermann, 1982), which corresponds to fraction 8 in Fig. 6A. Since the majority of N protein was present in fractions 5–6, the data indicate that virus particles were likely produced but that they were slightly lighter than the infectious virus, suggesting some kind of defects with the virus particles. One possibility for a lower buoyant density is the lack of viral genomic RNA, i.e. virus-like particles. However, since the N protein is associated with the genome, the detection of N protein in the viral fractions argues against this possibility, although N protein can also interact with M protein during assembly (Narayanan et al., 2000). Nevertheless, to experimentally demonstrate this possibility, fractions

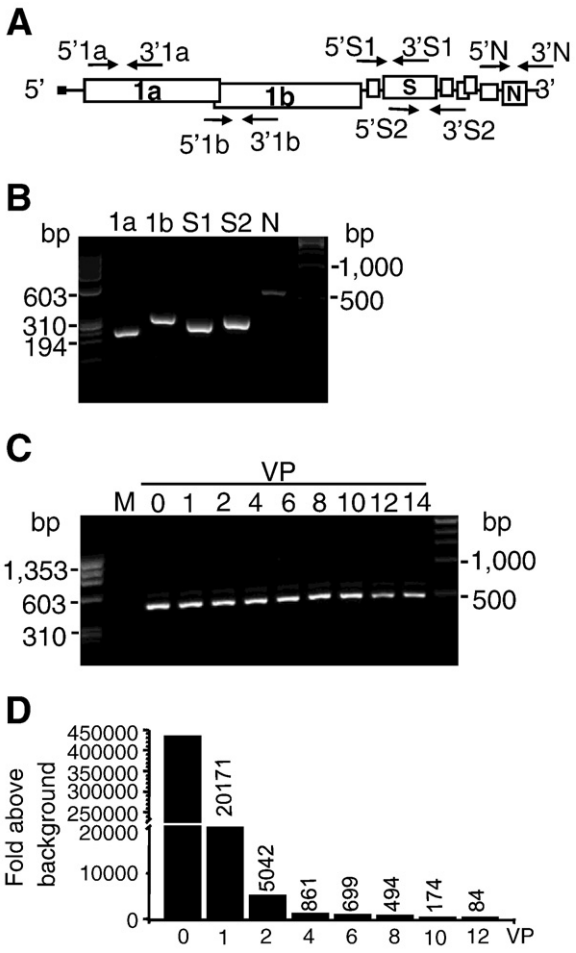

Fig. 2. Persistence of viral genomic RNAs in N20.1 cells. (A) Schematic diagram showing viral genome organization with highlight of genes 1a/1b, S and N, and the relative locations (arrows) and names of the primer pairs used in the RT-PCR detection. (B) Detection of viral RNA genome in persistently infected N20.1 cells at passage 4 (VP4). Five RT-PCR products (1a, 1b, S1, S2, and N) represent the 5 regions throughout the viral genome as shown in (A). Unmarked lanes on both sides are molecular weight marker in base pair (bp). (C) Detection of viral genomic RNA at various passages (VP0–VP14) of the persistently infected N20.1 cells. The RT-PCR product corresponds to the region within the N gene as shown in (A). M, mock-infected cells as a negative control. Molecular weight markers are shown on both sides in bp. (D) Real-time quantitative RT-PCR detection of viral genomic RNA at various passages (VP0–VP12). The number represents the relative amount of viral genomic RNA (fold) above the background.

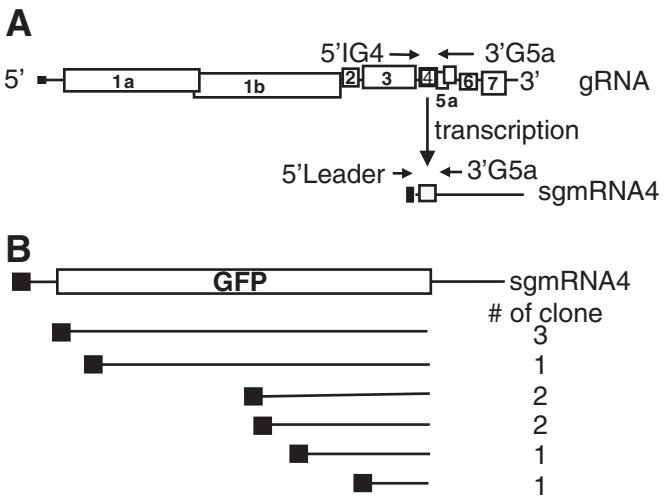

Fig. 3. Loss of GFP expression is associated with aberrant transcription of subgenomic mRNA4 coding for GFP in persistently infected N20.1 cells. (A) Schematic diagram showing viral genome (gRNA) organization and transcription of subgenomic (sg) mRNA4, the relative locations (arrows) and names of the primer pairs used in the RT-PCR. (B) Schematic diagram showing various species of sgmRNA4 identified by sequencing. The mRNAs have a leader RNA fused with the body sequence at various locations within the GFP open reading frame. A total of 10 clones of the RT-PCR products were sequenced. The number of clones representing each mRNA species is shown on the right.

5 to 10 were combined. RNAs were then extracted for RT-PCR with primers specific to viral genome within the N gene-coding region. Indeed, specific viral genomic RNAs were detected in the purified fractions from persistently infected N20.1 cells (Fig. 6B, lane VP) and in virus samples derived from acutely infected 17Cl-1 cells that served as a positive control (Fig. 6B, lane V). Viral RNAs were not detected in samples derived from mock-infected N20.1 or 17Cl-1 cells (Fig. 6B). These results confirm that viral genomes were present in the fractions that represent viral particles.

We next determined the viral structural proteins in the purified "virions". We used antibodies to viral S, N, and E proteins in Western blot. As shown in Fig. 6C, all these viral structural proteins were detected. However, in comparison with the viruses propagated in 17Cl-1 cells, the amount of S protein was very low relative to the amount of N protein. We also noticed that the amount of S protein expressed in the persistently infected cells was extremely low at late passages (Fig. 4E). It is worth noting that due to the absence of infectivity for virion isolated from persistent cells, it was not possible to precisely quantify the virion protein by loading an equivalent PFU. Thus, the ratio of envelope proteins (S and E) to N protein was used as a measure for describing the relative amount of envelope protein per physical particle. In addition, the species of the virion S protein from persistently infected N20.1 cells appeared to be different from that from acutely infected 17Cl-1 cells. Similar phenomenon was also observed between the S proteins in acutely and persistently infected cells (compare with Fig. 4E). However, it remains to be seen whether this is due to differential glycosylation or other post-translational modifications. The E protein from persistently infected N20.1 cells appeared less abundant compared to that from 17Cl-1 cells (Fig. 6C, lower panels). We also detected the M protein from persistently infected N20.1 cells and 17Cl-1 cells; however, due to high background, we were unable to compare its relative amount in different cell types (data not shown).

Morphological features of the virions isolated from persistently infected oligodendrocytes

The detection of viral structural proteins and RNA genome in the purified sucrose gradient fractions in above experiments indicates that virions were likely assembled. However, the absence of infectivity prompted us to examine the morphology of the viral particles. Thus, purified virus preparations were subjected to negative-staining followed by electron microscopic examination. In general, diverse morphology of the virions had been observed in each grid for the same sample (Fig. 7). The shape and size of the virions isolated from acutely or persistently infected N20.1 cells and from 17Cl-1 cells were indistinguishable. Interestingly, however, little to no spike was found on the virions isolated from persistently infected N20.1 cells (panels a–b). In contrast, virions isolated from acutely infected N20.1 or 17Cl-1 cells exhibited the typical "crown" morphology of the coronavirus, i.e. the spike protein protruding from the virion surface to form a ring (panels c–e). Thus, it appears that the only obvious morphological distinction between infectious and non-infectious virions is the presence or abundance of the spike protein on virion surface observed under EM examination.

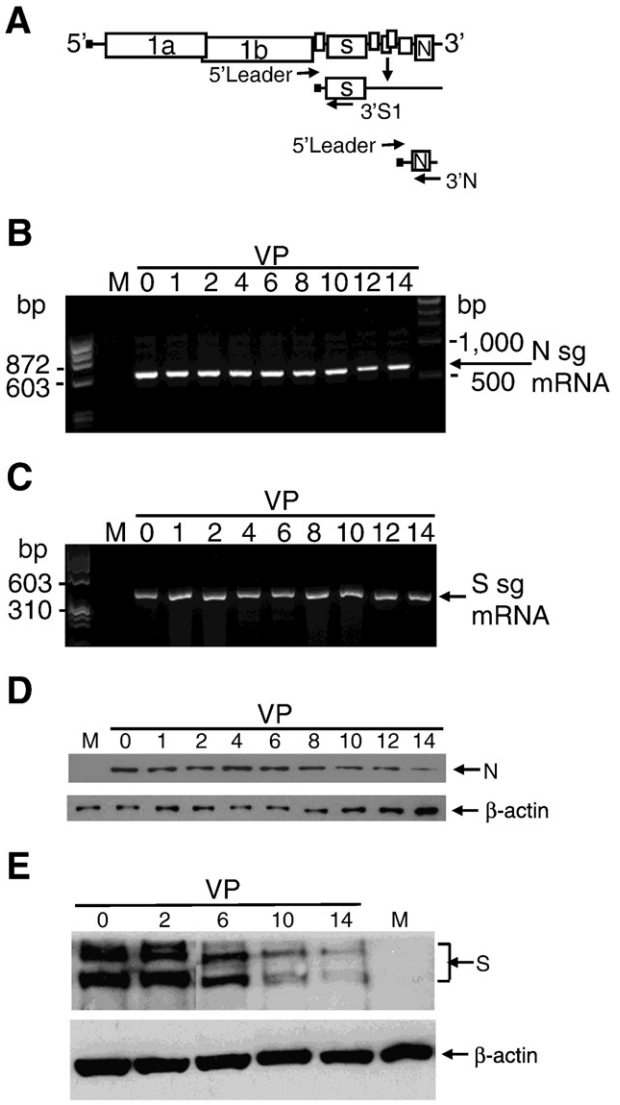

Fig. 4. Expression of viral genes in persistently infected N20.1 cells. (A) Schematic diagram showing viral genome organization with highlight of genes 1a/1b, S and N, the subgenomic mRNAs for the S and N genes, and the relative location and name of the primer pairs used in the RT-PCR. (B and C) Detection of subgenomic mRNAs for N and S genes, respectively, in acutely and persistently infected N20.1 cells at various passages (VP0–VP14). M, mock-infected cells as a negative control. Molecular weight marker is shown on the left in base pair (bp). (D and E) Detection of viral N and S protein, respectively, in acutely and persistently infected N20.1 cells at various passages (VP0–VP14) by Western blot analysis. M, mock-infected cells as a negative control. β-Actin was used as an internal control for protein loading.

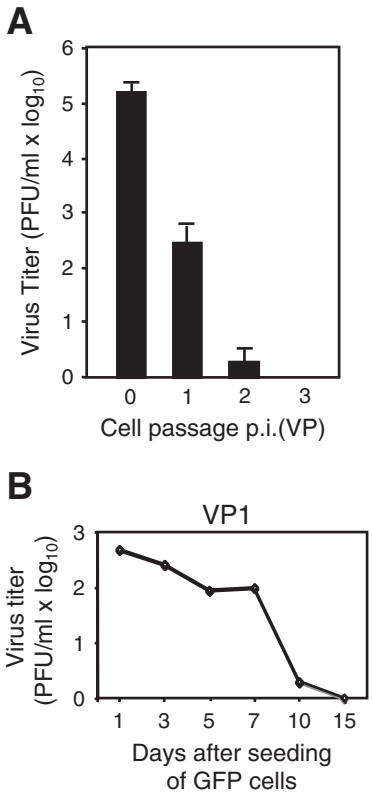

Fig. 5. Loss of viral infectivity in persistently infected N20.1 cells. (A) Determination of viral infectivity in acutely and persistently infected N20.1 cells. N20.1 cells were infected with MHV-A59/GFP at an m.o.i. of 10. Culture medium and cell lysates were collected at 48 h p.i. (VP0) or 48 h after each passage (VP1–VP3). Virus titer was determined by plaque assay on DBT cells. The results are expressed as the mean PFU per ml for three independent experiments. Error bars indicate standard deviations of the means. (B) Virus titers in cultures at various days after seeding of the GFP-positive cells (VP1). The results are expressed as an average PFU per ml of two samples for each time point.

Lack of evidence for mutations in the interacting domains of the viral envelope proteins during persistence in oligodendrocytes

It has been suggested that incorporation of S protein into virion envelope requires the interaction between S and M proteins, more specifically between the transmembrane and amphipathic domains of M protein and the carboxyl-terminal domain of the S protein (Fig. 8A) (de Haan et al., 1999; de Haan and Rottier, 2007). While the E protein is not absolutely required for replication, lack of E drastically reduces viral replication and fitness (Kuo and Masters, 2003). Thus, to gain an insight into potential defects associated with S protein incorporation, we determined whether any mutations in the carboxyl-terminal domain of S protein or M and E proteins arisen during persistence might contribute to the lack of incorporation. We amplified a sequence at the 3′-end of S gene that encodes the carboxyl-terminal domain of the S protein (including the transmembrane domain and cytoplasmic tail) from various passages of persistently infected N20.1 cells (Figs. 8B and C). We also amplified the entire ORFs of the M and E gene from acutely (VP0) and persistently infected N20.1 cells at passages 10 (VP10) and 16 (VP16) (Figs. 8B and C). Direct sequencing of the RT-PCR products (Fig. 8C) revealed that there was no single nucleotide mutation at the 3′-end of the S gene and within the ORF for M and E genes (data not shown). These results suggest that deficient incorporation of S protein in the virions during persistence unlikely results from lack of interactions among envelope proteins due to mutations in the interacting domains.

Discussion

The hallmark of MHV persistent infection in the animal CNS is the persistence of viral genome without the detection of infectious viruses (Bergmann et al., 2006). To recapitulate this in vivo phenomenon it would be highly desirable to have a robust in vitro cell culture system, such that the molecular mechanisms of viral persistence can be carefully examined at the cellular level. In an effort to achieve that objective, over the past decades we and others have searched a large number of susceptible cell lines and primary cell cultures for their potential as hosts for MHV persistence. Although these investigations have established MHV persistence in many types of cells following various manipulations of culture conditions, persistently infected cells continue to produce infectious viruses (Chen and Baric, 1996; Lavi et al., 1987; Sawicki et al., 1995; Schickli et al., 1997). Only the rat progenitor oligodendrocyte CG-4 cell line has been reported to harbor MHV genomes without producing infectious viruses (Liu and Zhang,

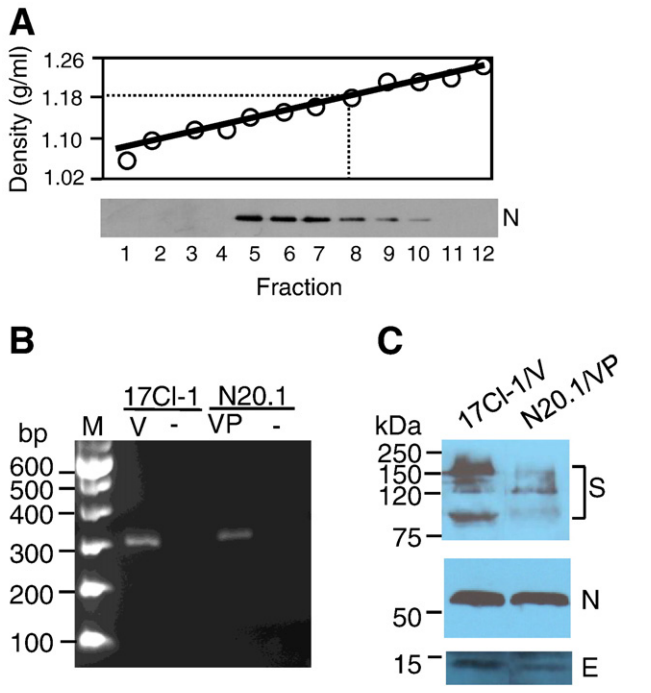

Fig. 6. Biophysical and biochemical characterization of virus preparations isolated from persistently infected N20.1 cells. (A) Determination of virus buoyant density. Following purification of the virus preparations, the sucrose gradient was fractionated and the buoyant density (g/ml) for each fraction was determined and plotted (see Materials and methods). The presence of virus in each fraction was further determined by Western blot analysis using a mAb specific to viral N protein. The dashed line indicates the standard buoyant density (1.18–1.19 g/ml) for coronaviruses as a reference. (B) Presence of viral genomic RNA in the purified viral preparations. RNAs were isolated from gradient-purified fractions. RT-PCR was performed to detect viral genomic RNAs (VP). Preparations from mock-infected N20.1 cells or 17Cl-1 cells were used as a negative control while preparation from acutely infected 17Cl-1 cells (V) was used as a positive control. Arrow indicates the unique RT-PCR product representing viral RNA. (C) Presence of viral structural proteins in the gradient-purified virus preparations from persistently infected N20.1 cells was determined by Western blot using antibodies to MHV S, N and E proteins. Virus preparations from acutely infected 17Cl-1 cells were purified in parallel and used as a positive control.

2005). However, in that study it was not clear whether all cells had been infected with MHV (Liu and Zhang, 2005). It is more likely that only a small population of cells were initially infected with MHV or were permissive for MHV replication, because less than 1% of the infected cells exhibited strong fluorescence when stained with an antibody specific to MHV N protein (Liu et al., 2003). This suggests that only a tiny fraction of the cells may persistently harbor the virus. In the present study, we employed a recombinant MHV that expresses GFP. This improvement allows us to screen multiple cell lines for their susceptibility to MHV infection and to identify and isolate infected cells. Indeed, we found that ≈25% of N20.1 cells exhibited strong GFP expression (Fig. 1). Subsequent FACS sorting and subcultures of the GFP-positive N20.1 cells led to the establishment of persistent infection without production of infectious viruses (Figs. 1–4), which recapitulates the phenomenon observed in mouse CNS. Thus, establishment of such a faithful system paves the foundation for future mechanistic studies of MHV persistence in CNS cells.

Ironically, non-productive persistence is established only in 3 cell lines of oligodendrocytic origin (mouse oligodendrocyte N20.1 and Oligo-neu (this study) and rat progenitor oligodendrocyte CG-4 (Liu and Zhang, 2005)) in spite of different conditions used for establishing these cell lines. This raises a possibility that this kind of MHV persistence is cell-type specific. CG-4 cell is a permanent, undifferentiated type 2 oligodendrocyte/astrocyte progenitor cell that was originally established during a primary neural cell culture derived from the brain of newborn (1–3 days postnatal) Sprague–Dawley rat pups (Louis et al., 1992). It is maintained at the progenitor state under complex culture conditions containing various growth factors. It can differentiate into mature oligodendrocyte upon changing culture conditions. N20.1 cell is a cell line clone derived from mouse primary cultures of oligodendrocytes conditionally immortalized by transformation with a temperature-sensitive mutant of the simian virus 40 large-T antigen (Verity et al., 1993). The Oligo-neu is a murine oligodendroglial precursor cell line established via transformation of a replication-defective retrovirus expressing t-neu oncogene linked to the external region of the human epidermal growth factor receptor (Jung et al., 1995). Although the 3 cell lines were derived from different animal species and were established by different methods, they appear to retain the susceptibility to non-productive persistence by MHV. This is in stark contrast to fibroblast (17Cl-1) and astrocytoma (DBT) cell lines (Chen and Baric, 1996; Sawicki et al., 1995), where infectious virus continues to generate. Another difference between the non-productive persistence in N20.1 cells and the productive persistence in fibroblast and astrocytoma cell lines is that persistence can be established only in mixed (infected and uninfected; susceptible and resistant) cultures of 17Cl-1 and DBT (Chen and Baric, 1996; Sawicki et al., 1995). In such mixed cultures with low multiplicity of infection, a small number of viruses released from a small fraction of cell populations can infect neighboring uninfected cells and thus the persistence can be maintained in an epigenetic fashion (Sawicki et al., 1995). The persistence in N20.1 cells was established following selection of infected cells. When GFP-expressing 17Cl-1 or DBT cells were selected by the same FACS sorting following infection with MHV-A59/GFP, continuous passaging of the GFP-expressing 17Cl-1 and DBT cells was not possible, due to extensive cell death for 17Cl-1 as described by Chen and Makino (2002) or extensive cell fusion for DBT cells. However, it has been reported that infectious virus continued to produce in persistently infected primary mouse oligodendrocytes (Lavi et al., 1987). One possible reason for the observed difference between primary oligodendrocytes and established oligodendroglial cell lines is that primary oligodendrocytes cannot be subcultured for many passages, thus leaving insufficient time for eventual cease of infectious virus production to take place. Another possibility is that culture conditions used for primary cells and cell lines might be different, which can affect cell proliferation and differentiation, which in turn affect virus replication and infectious virus production. A third possibility is that most primary cultures have a certain degree of impurity, i.e., contamination with a small number of astrocytes and microglia that can serve as a reservoir for infectious virus production, albeit at a low level.

One of our initial purposes to use the GFP-expressing virus was to continuously monitor progression of the persistent infection. However, the eventual disappearance of GFP-positivity is unexpected. Interestingly, while aberrant transcription of subgenomic mRNA for GFP gene, a phenomenon reminiscent of the aberrant transcription described previously for MHV (Fischer et al., 1997; Zhang and Lai, 1994), was identified (Fig. 3), subgenomic mRNAs coding for viral structural proteins such as S, E, M, and N were transcribed with no apparent abnormality; further Western blot analyses confirmed the expression of these viral structural proteins (Figs. 2 and 4 and further data not shown). Thus, it appears that MHV has the ability to selectively inactivate the GFP gene expression through aberrant transcription while keeping viral own genes continuously expressed. Why and how MHV can discriminate self from non-self during gene expression remain an interesting subject for future investigation.

It has been known for decades in the coronavirus research field that MHV can establish persistent infection in the mouse CNS without apparent production of infectious viruses. This kind of so-called non-productive persistence is unique among animal viruses. The most intriguing question remained to be answered, however, is what the major defects in the virus life cycle are associated with the non-productive persistence. Despite the enormous technical challenges on studying persistent infection, our comprehensive biophysical,

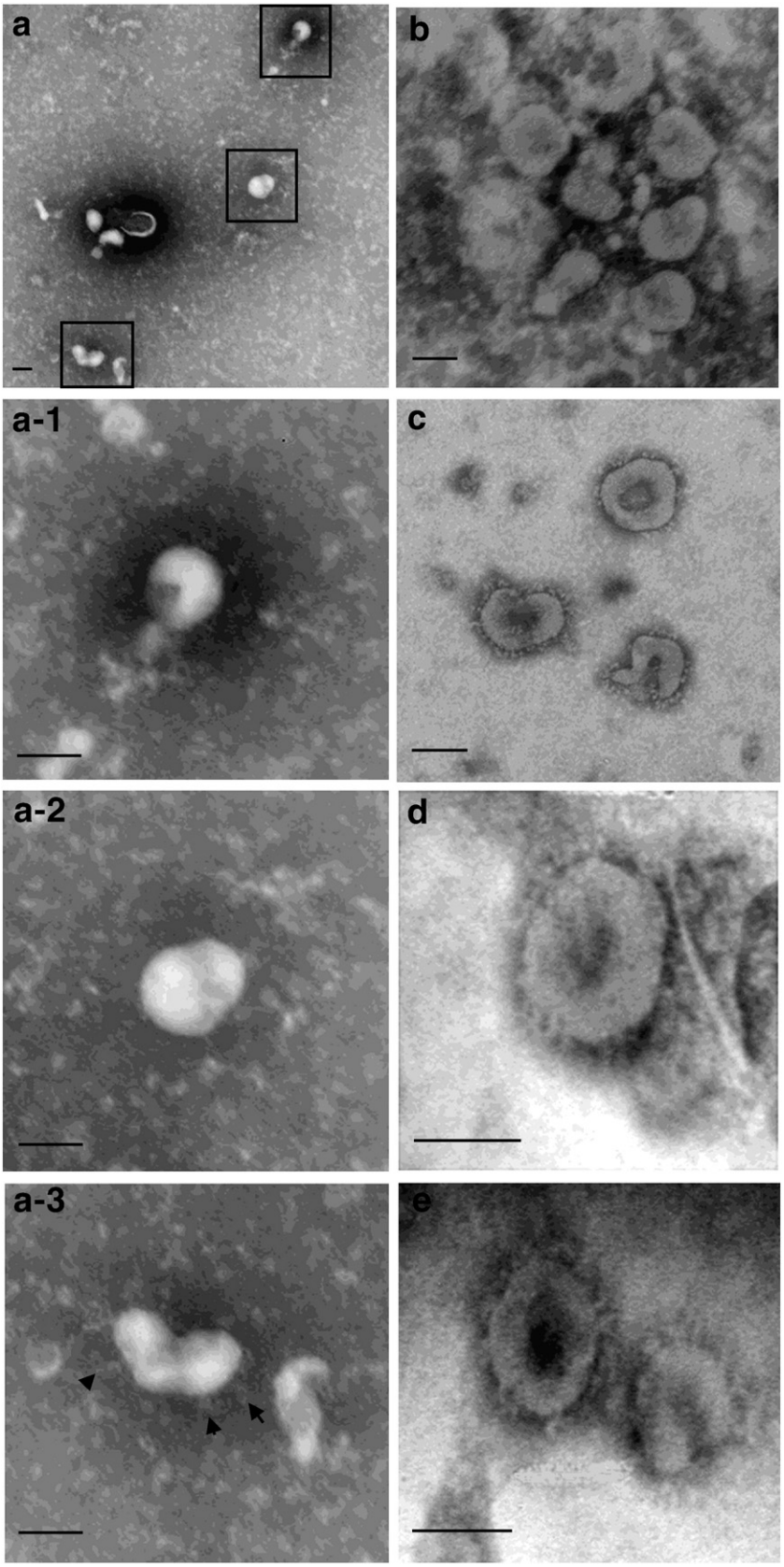

Fig. 7. Deficient incorporation of spike protein in viral particles isolated from persistently infected N20.1 cells. (a–b) Negative-stain electron micrographs of viral particles isolated from persistently infected N20.1 cells, showing a lack or deficiency of spikes. Panels a1–a3 are higher magnification images of viral particles shown in (a). The arrows in a3 indicate possible "spikes". (c) EM images for virions isolated from acutely infected N20.1 cells, showing the typical crown-like spikes. (d–e) EM images for virions isolated from acutely infected 17Cl-1 cells, showing the spikes protruding from virion surface. The size bar indicates 100 nm.

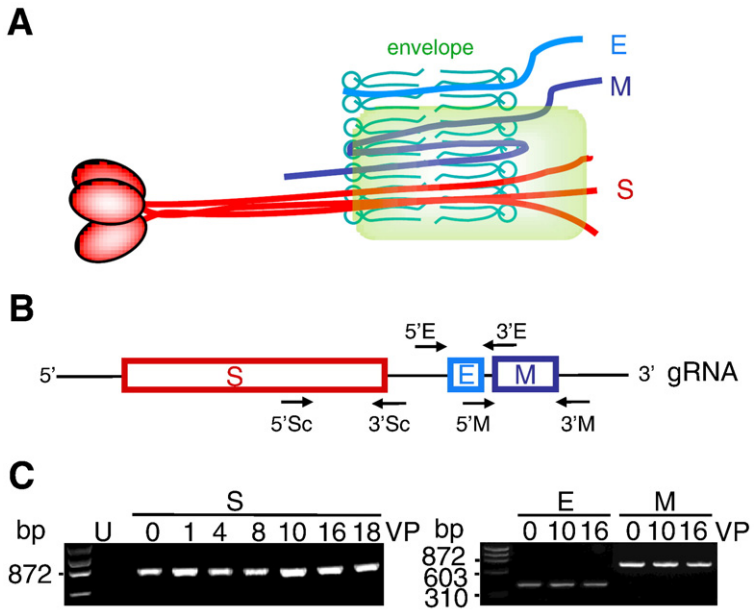

Fig. 8. Analysis of virion envelope genes from persistent N20.1 cells. (A) Membrane topology of MHV-A59 envelope proteins. The rectangular shade highlights the transmembrane and C-terminal domains of S and M proteins involved in interaction and spike incorporation during virion assembly. (B) Diagram showing S, M and E genes in viral genomic RNA and the location and name of the primer pairs used in RT-PCR. (C) Agarose gel showing the RT-PCR products of viral S, M, and E genes from various passages of the persistently infected N20.1 cells (VP). VP0 indicates RNA samples isolated from acute infection at 48 h p.i.; U, uninfected. Molecular weight marker is shown in base pair (bp).

biochemical and EM analyses have identified a potentially key defect in the virus life cycle, which may contribute to the lack of viral infectivity. We found that viral genomic RNAs continuously replicate, that subgenomic mRNAs are transcribed, and that viral structural proteins are expressed in persistently infected N20.1 cells. Successful continuation of these processes likely contributes to the maintenance of viral persistence. However, we also found that while viral particles are assembled in the persistently infected cells (Figs. 6 and 7), these virions are not infectious upon infection of susceptible DBT cells (data not shown), although continuous blind passage of "infected" DBT cells has not been carried out. The most likely reason for a lack of infectivity of these virions is deficiency in incorporation of viral spike protein into the viral envelope, since spike protein is the key determinant for coronavirus infectivity. This is evidenced with the EM examination, which shows that virions isolated from persistently infected cells scarcely have spikes protruding from virion surface. Although the spike sometimes can get lost following the purification procedures, the overwhelming presence of spikes in virions isolated from acutely infected N20.1 or 17Cl-1 cells, which have been subjected to the same purification procedures in parallel experiments, suggests that the deficiency in spike incorporation into persistent viral particles is not simply caused by technicality; rather it is more likely due to some kind of defects in virion assembly. However, since virions from acutely infected N20.1 cells are infectious and have abundant spikes (Fig. 7, d–e), this finding suggests that defective incorporation of spike protein may have occurred following the establishment of persistent infection.

What caused defective incorporation of spike protein? Since there are no apparent mutations in virion envelope proteins (Fig. 8) associated with S incorporation (de Haan et al., 1999; de Haan and Rottier, 2007), we hypothesize that some cellular factors that are triggered by MHV infection and persistence might in turn inhibit spike protein incorporation into virions. It has been reported that treatment of cells with type I interferon (IFN) significantly inhibited the glycosylation of vesicular stomatitis virus (VSV) G protein, the incorporation of G protein into virions and the virus infectivity (Maheshwari et al., 1980a,b; Jay et al., 1983). It has also been shown that inhibition of glycosylation of MHV S protein by the drug tunicamycin led to retention of unglycosylated S protein in the endoplasmic reticulum (ER), prevented S protein from incorporation into virions and resulted in production of spikeless virions and loss of viral infectivity (Holmes et al., 1981; Rottier et al., 1981). Similarly, infection with two temperature-sensitive mutants of MHV-A59 resulted in lack of the mature Golgi form and oligomerization of S, retention of the S in the ER, and lack of S in purified virions produced at the non-permissive temperature (Luytjes et al., 1997). A mutant isolated from DBT cells persistently infected with MHV-JHM strain exhibited slightly lower buoyant density and had fewer spikes; although the mutant replicated slower (small plaque mutant), it was nevertheless infectious (Makino et al. 1983). Interestingly, type I IFN is induced in N20.1 cells by MHV infection and pretreatment of N20.1 cells with IFNs inhibited MHV infectivity (Li et al., 2010). Coincidently, there is apparent deficiency of a higher molecular weight (possibly glycosylated) S protein from IFN-producing, persistent N20.1 cells as compared to that from IFN-nonproducing 17Cl-1 cells (Fig. 6C). Thus, we speculate that, like VSV G protein, IFNs and possibly other cellular factors that are induced by MHV infection in N20.1 cells subsequently inhibit virus infectivity by blocking the incorporation of S protein into virions during assembly. Such a possibility is currently under intense investigation.

Materials and methods

Cells and virus

The N20.1 cell is a cell line clone derived from mouse primary cultures of oligodendrocyte conditionally immortalized by transformation with a temperature-sensitive mutant of the simian virus 40 large-T antigen (Verity et al., 1993). It was kindly provided by Dr. Anthony Compadre (University of California Los Angeles School of Medicine). The N20.1 cell represents a mature oligodendrocyte because it expresses the myelin basic protein (MBP) and myelin proteolipid protein (PLP), but one that is at a very early stage of maturity based on the expression of the MBP and PLP alternatively spliced mRNA population (Verity et al., 1993). In addition, the N20.1 cell can be recognized by the A2B5 antibody, which recognizes a surface galactolipid expressed by oligodendrocyte progenitor cells; the A007 antibody, which is specific for sulfatide and found on cells

committed to the oligodendrocyte lineage as well as mature oligodendrocytes, and the anti-GC antibody, which recognizes the protein expressed specifically by mature oligodendrocytes (Verity et al., 1993). The N20.1 cells were cultured in Dulbecco's modified Eagle's medium (DMEM)/F12 with 10% fetal bovine serum (FBS) and G418 (100 μg/ml) at the permissive temperature of 34 °C. Cells were grown either in T25 flasks or Petri dishes. The mouse oligodendroglial precursor cell line Oligo-neu was kindly provided by Dr. Patricia Wight (UAMS) with permission from Dr. Jacalyn Trotter (University of Heidelberg, Germany). Mouse fibroblast 17Cl-1 cells (kindly provided by Dr. Susan Baker, Loyola University of Chicago Medical Center) were cultured in DMEM. Mouse astrocytoma DBT cells were cultured in Eagle minimal essential medium (EMEM) and were used for virus propagation and plaque assay as described previously (Liu et al., 2003). The recombinant mouse hepatitis virus (MHV)-A59/GFP expresses the green fluorescence protein (GFP) that replaced the viral nonstructural protein 4 (NS4) (kindly provided by Dr. Susan Weiss, University of Pennsylvania School of Medicine). The virus was propagated in DBT cells or 17Cl-1 cells.

Fluorescence-assisted cell sorting (FACS)

Following infection of N20.1 cells with MHV-A59/GFP at a multiplicity of infection (m.o.i.) of 10, cells were observed for GFP expression, which began at around 12 h p.i. and increased with time. When strong GFP expression was observed (at ≈48 h p.i.), cells were trypsinized and prepared for FACS with the FACS ARIA (BD Bioscience) in the departmental flow cytometry core facility. Cells were sorted into fluorescence-positive and -negative groups, which were then re-seeded separately for further study.

RNA isolation and conventional or real-time quantitative reverse transcription-polymerase chain reaction (qRT-PCR)

For detection of viral RNAs in infected cells, intracellular total RNAs were isolated from N20.1 cells using the Qiagen RNeasy plus Mini kit (Cat.#74134) according to the manufacturer's protocol and treated with RNase-free DNase I (Qiagen). The concentration of the RNA samples was determined with a spectrophotometer (Model U2001, Hitachi). For detection of viral genome and mRNAs, conventional RT-PCR was carried out as described previously (Liu and Zhang, 2005). The following primer pairs were used for detecting viral genomic RNA: The forward primer 5′ 1a (5′-TGT GCC GAG TGA TGA GAC GCA-3′) and reverse primer 3′1a (5′-GCC ACA TAA CCA CCT TGT GGA AGG A-3′) for detecting gene 1a at nt positions 3503–3742 (239 nt in length); 5′1b (5′-TGT GTA GGC ACA GGC TCC CAG T-3′) and 3′1b (5′-CGT GTT CAG CCA CAA CAC CGC-3′) for gene 1b at nt positions 1368–13891 (323 nt in length); 5′S1 (5′-GCT TGT GAA TTC AAA CGG TGC TAA TGT-3′) and 3′S1 (5′-TGC AGT TGC ACC TGA TGG CGT-3′) for S1 gene at nt positions 23997–24291 (294 nt in length); 5′S2 (5′-GCT GGG TGC TAT CCA GGA TGG GT-3′) and 3′S2 (5′-CGC GTG GTT TGG CTC TTA ACG C-3′) for S2 at nt positions 26868–27194 (326 nt in length); 5′N (5′-ATG GAA TCC TCA AGA AGA-3′) and 3′ N (5′-CCT GAG GCA ATA CCG TGC-3′) for N gene (500 nt in length). The primer pairs: 5′Leader (5′-TTATAAGAG GATTGGCGTCCG-3′) and 3′S1, and 5′Leader and 3′N were used to amplify the S (400 nt) and N (576 nt) subgenomic mRNAs, respectively. In addition, the primer pair NF43 (5′-TCC TCT GTA AAC CGC GCT GGT AAT-3′) and NR370 (5′-GCA GTA ATT GCT TCT GCT GCC CAT-3′) was used for amplifying virion genomic RNA corresponding to the sequence (328 nt) within the N gene shown in Fig. 6. Primer pair 5′IG4 (5′-TTG ACT ATC ACA GCC TCT CC-3′, which is located upstream of gene 4 and starts at nt 27901) and 3′-G5a (5′-GGC ATG TGA GTG ATG CAT GG-3′, which is located within gene 5a at nt 28420) was used for amplifying gene 4 (GFP) from viral genomic RNA and primer pair 5′Leader and 3′G5a for subgenomic mRNA4 (GFP). The following primer pairs were used for amplifying the 3′-end of S gene, and the full-length of M and E genes, respectively: 5′Sc (5′-CTC GGC TTG AGG CTG TAG AAG C-3′, nt 27023) and 3′Sc (5′-ACA TGA GCC ACA ACC TGT GCA GC-3′, nt 27813); 5′M (5′-TGA GAC TGC CCC TAT TAG AGG TGG A-3′, nt 28923) and 3′M (5′-GAG GAG CTT CTG CCA CCG GC-3′, nt 29715); 5′E (5′-CGG CAG AAC TGT CCA ACA GGC C-3′, nt 28620) and 3′E (5′-TTG AAC TGC CTC GTG GGC CG-3′, nt 29030). The PCR products were analyzed by agarose gel electrophoresis.

For qRT-PCR, 1 ng of the total RNA sample was used in RT reaction (25 μl) using the iScript cDNA synthesis kit (Bio-Rad Laboratories) according to the manufacturer's instruction. The reaction was carried out in an Applied Biosystems 9800 ThermoCycler in a 96-well plate for 5 min at 25 °C, 30 min at 42 °C, and 5 min at 85 °C and was then held at 4 °C. Real-time qPCR was carried out in 50 μl reaction mixture containing 1 μl RT product, 1× iQ SYBR Green Supermix PCR master mix and 100 nM primers using an iCycler IQ Multicolor Real-time PCR Detection system (Bio-Rad). The primer pair 5′qPCR (5′-TGC TTG GCT TTC ACA CTT TGT CCC-3′) and 3′qPCR (5′-ACC CAC TGG ATA CCA GGC TGA CAA-3′) amplifies a 172-nt fragment of the viral genomic RNA between nt 11402 and 11574. The PCR was performed in a 96-well optical plate at 95 °C for 10 min, followed by 40 cycles of 95 °C for 15 s and 57° for 1 min. Results were analyzed using the iCycler IQ multicolor real-time PCR detection system (Bio-Rad Laboratories). Gene expression levels in various experimental groups were calculated after normalizing cycle thresholds against the housekeeping gene β-actin (using primer pair 5′b-actin: 5′-ACA GCT TTA CCA CCA CTG CTG AGA-3′ and 3′b-actin: 5′-AGG AAG ATG ATG CAG CAG TAG CCA-3′) and are presented as fold increase above the background from mock-infected cells. The threshold cycle (Ct) is defined as the fractional cycle number at which the fluorescence passes the fixed threshold. Relative gene expression values were determined using the $2^{-\Delta\Delta CT}$ method of Livak and Schmittgen (2001).

Western blot analysis

For Western blot analysis, whole cell lysates were prepared using cell lysis buffer (Cat.#9038, Cell Signaling Inc.) according to the manufacturer's protocol. The protein concentration was determined by using Bio-Rad protein assay kit. Equal amounts of total proteins were resolved by sodium deoxyl sulfate-polyacrylamide gel electrophoresis (SDS-PAGE) and transferred onto nitrocellulose membrane (Bio-Rad) for 7 h at 40 V in the transfer buffer. Membranes were blocked for 1 h at room temperature with 5% powdered skim milk in Tris-buffered saline (10 mM Tris–Cl [pH 7.5], 150 mM NaCl) with 0.05% Tween 20 (TBST). The membranes were incubated with a primary antibody at 4 °C overnight, followed by incubation with a secondary horseradish-peroxidase (HRP)-conjugated antibody (Sigma) for 1 h at room temperature. Blots were developed with Pierce® ECL Western Blotting Substrate and detection system (Thermo-Fisher Scientific) and exposed to X-ray film (Fuji). After the membranes were incubated in stripping buffer (10 mM ß-mercaptoethanol, 2% (w/v) SDS, and 62.5 mM Tris, pH 6.7) at 55 °C for 30 min, they were washed in TBST, blocked, and incubated with anti-β-actin mAb (as an internal control) at room temperature for 1 h. Detection of β-actin was carried out following incubation with the secondary anti-mouse IgG antibody conjugated with HRP and ECL. The following antibodies were used in this study: A goat antibody against MHV-A59 spike protein (termed A04), a goat antibody specific to MHV E protein, and a mouse monoclonal antibody to MHV N protein, which were kindly provided by Drs. Kathryn Holmes (University of Colorado School of Medicine at Denver, CO), Julian Leibowitz (University of Texas A&M, Health Science Center at College Station, TX) and John Fleming (University of Wisconsin Medical Center at Madison, WI), respectively.

Virus purification and buoyant density determination

Virus preparation was purified from the cultured medium through a 30% (w/v) sucrose cushion by ultracentrifugation at 27,000 rpm at 4 °C for 4 h in the SW28 rotor (Beckman Coulter). Virus pellets were

resuspended in phosphate-buffered saline (PBS) and were further purified through 10–70% (w/v) sucrose gradient by ultracentrifugation at 35,000 rpm at 4 °C overnight in an SW40 rotor (Beckman Coulter). The gradient was then fractionated into 12 fractions. The density of each fraction was determined with a refractometer and was further confirmed with the simple weight and volume determination, i.e. the weight of 100 μl of each fraction. The density was then plotted as gram per milliliter.

Negative contrast electron microscopy

Negative contrast electron microscopy was carried out as described previously (Zhang et al., 1994). Briefly, formvar-coated copper grids were floated for 15 min on drops of the concentrated virus suspension, dried by lightly touching with filter paper and washed 1–2 times in deionized water. Subsequently the grids were stained by floating for 1 min on drops of 1% phosphotungstate acid in PBS, and examined with a ZEISS EM10/CR electron microscope (EM) at 60–80 kV.

Acknowledgments

We thank Dr. Anthony Compadre (University of California at Los Angeles School of Medicine, Los Angeles) for kindly providing the N20.1 cells, Dr. Susan Weiss (University of Pennsylvania School of Medicine, Philadelphia) for the recombinant MHV-A59/GFP, Dr. Kathryn Holmes (University of Colorado Health Science Center, Denver, Colorado) for antibodies to MHV-A59 spike and membrane proteins, Dr. Julian Leibowitz (University of Texas A&M Health Science Center, College Station, Texas) for antibody to MHV envelope protein, and Dr. John Fleming (University of Wisconsin Medical Center, Madison, Wisconsin) for antibody to MHV nucleocapsid protein. This work was supported by Public Health Service grant NS047499 and in part by the P30 core grant NS047546 and grant AI061204 from the National Institutes of Health.

References

Bergmann, C.C., Lane, T.E., Stohlman, S.A., 2006. Coronavirus infection of the central nervous system: host–virus stand-off. Nat. Rev. Microbiol. 4, 121–132.
Boyle, J.F., Weismiller, D.G., Holmes, K.V., 1987. Genetic resistance to mouse hepatitis virus correlates with the absence of virus binding activity on target tissues. J. Virol. 61, 185–189.
Chambers, P.C., Pringle, R., Easton, A.J., 1990. Heptad repeat sequences are located adjacent to hydrophobic regions in several types of virus fusion glycoproteins. J. Gen. Virol. 71, 3075–3080.
Chen, W., Baric, R.S., 1996. Molecular anatomy of mouse hepatitis virus persistence: coevolution of increased host cell resistance and virus virulence. J. Virol. 70, 3947–3960.
Chen, C.J., Makino, S., 2002. Murine coronavirus-induced apoptosis in 17Cl-1 cells involves a mitochondria-mediated pathway and its downstream caspase-8 activation and bid cleavage. Virology 302, 321–332.
Collins, A.R., Knobler, R.L., Powell, H., Buchmeier, M.J., 1982. Monoclonal antibodies to murine hepatitis virus-4 (strain JHM) define the viral glycoprotein responsible for attachment and cell–cell fusion. Virology 119, 358–371.
Dandeker, A.A., Perlman, S., 2002. Virus-induced demyelination in nude mice is mediated by gd T cells. Am. J. Pathol. 161, 1255–1263.
Das Sarma, J., Fu, L., Tsai, J.C., Weiss, S.R., Lavi, E., 2000. Demyelination determinants map to the spike glycoprotein gene of coronavirus mouse hepatitis virus. J. Virol. 74, 9206–9213.
Das Sarma, J., Scheen, E., Seo, S.-H., Koval, M., Weiss, S.R., 2002. Enhanced green fluorescent protein expression may be used to monitor murine coronavirus spread in vitro and in the mouse central nervous system. J. Neurovirol. 8, 1–11.
de Groot, R.J., Luytjes, W., Horzinek, M.C., van der Zeijst, B.A., Spaan, W.J., Lenstra, J.A., 1987. Evidence for a coiled-coil structure in the spike proteins of coronaviruses. J. Mol. Biol. 196, 963–966.
de Haan, C.A., Rottier, P.J., 2007. Molecular interactions in the assembly of coronaviruses. Adv. Virus Res. 64, 165–230.
de Haan, C.A., Smeets, M., Vernooij, F., Vennema, H., Rottier, P.J., 1999. Mapping of the coronavirus membrane protein domains involved in interaction with the spike protein. J. Virol. 73, 7441–7452.
de Haan, C.A., Stadler, K., Godeke, G.J., Bosch, B.J., Rottier, P.J., 2004. Cleavage inhibition of the murine coronavirus spike protein by a furin-like enzyme affects cell–cell but not virus–cell fusion. J. Virol. 78, 6048–6054.
Fischer, F., Stegen, C.F., Koetzner, C.A., Masters, P.S., 1997. Analysis of a recombinant mouse hepatitis virus expressing a foreign gene reveals a novel aspect of coronavirus transcription. J. Virol. 71, 5148–5160.
Fleming, J.O., Houtman, J.J., Alaca, H., Hinze, D., McKenzie, D., Aiken, J., Bleasdale, T., Baker, S., 1993a. Persistence of viral RNA in the central nervous system of mice inoculated with MHV-4. Adv. Exp. Med. Biol. 342, 327–332.
Fleming, J.O., Wang, F.I., Trousdale, M.D., Hinton, D., Stohlman, S.A., 1993b. Interaction of immune and central nervous systems: contribution of anti-viral Thy-1+ cells to demyelination induced by coronavirus JHM. Reg. Immunol. 5, 37–43.
Gallagher, T.M., Escarmis, C., Buchmeier, M.J., 1991. Alteration of the pH dependence of coronavirus-induced cell fusion: effect of mutations in the spike glycoprotein. J. Virol. 65, 1916–1928.
Holmes, K.V., Doller, E.W., Sturman, L.S., 1981. Tunicamycin resistant glycosylation of coronavirus glycoprotein: demonstration of a novel type of viral glycoprotein. Virology 115, 334–344.
Jay, F.T., Dawood, M.R., Friedman, R.M., 1983. Interferon induces the production of membrane protein-deficient and infectivity-defective vesicular stomatitis virions through interference in the virion assembly process. J. Gen. Virol. 64, 707–712.
Jung, M., Krämer, E., Grzenkowski, M., Tang, K., Blakemore, W., Aguzzi, A., Khazaie, K., Chlichlia, K., Von Blankenfeld, G., Kettenmann, H., Trotter, J., 1995. Lines of murine oligodendroglial precursor cells immortalized by an activated neu tyrosine kinase show distinct degrees of interaction with axons in vitro and in vivo. Eur. J. Neurosci. 7, 1245–1265.
Knobler, R.L., Dubois-Dalcq, M., Haspel, M.V., Claysmith, S.P., Lampert, P.W., Oldstone, M.B.A., 1981. Selective localization of wild type and mutant mouse hepatitis virus (JHM strain) antigens in CNS tissue by fluorescence, light and electron microscopy. J. Neuroimmunol. 1, 81–92.
Knobler, R.L., Lampert, P.W., Oldstone, M.B.A., 1982. Virus persistence and recurring demyelination produced by a temperature-sensitive mutant of MHV-4. Nature 298, 279–280.
Kubo, H., Yamada, Y.K., Taguchi, F., 1994. Localization of neutralizing epitopes and the receptor-binding site within the amino-terminal 330 amino acids of the murine coronavirus spike protein. J. Virol. 68, 5403–5410.
Kuo, L., Masters, P.S., 2003. The small envelope protein E is not essential for murine coronavirus replication. J. Virol. 77, 4597–4608.
Lai, M.M.C., Cavanagh, D., 1997. The molecular biology of coronaviruses. Adv. Virus Res. 48, 1–100.
Lane, T.E., Liu, M.T., Chen, B.P., Asensio, V.C., Samawi, R.M., Paoletti, A.D., Campbell, L.L., Kunkel, S.L., Fox, H.S., Buchmeier, M.J., 2000. A central role for CD4+ T cells and RANTES in virus-induced central nervous system inflammation and demyelination. J. Virol. 74, 1415–1424.
Lavi, E., Gilden, D.H., Wroblewska, Z., Rorke, L.B., Weiss, S.R., 1984. Persistence of mouse hepatitis virus A59 RNA in a slow virus demyelinating infection in m ice as detected by in situ hybridization. J. Virol. 51, 563–566.
Lavi, E., Suzumura, A., Hirayama, M., Highkin, M.K., Dambach, D.M., Silberberg, D.H., Weiss, S.R., 1987. Coronavirus mouse hepatitis virus (MHV)-A59 causes a persistent, productive infection in primary glial cell cultures. Microb. Pathog. 3, 79–86.
Li, J., Liu, Y., Zhang, X., 2010. Murine coronavirus induces type I interferon in oligodendrocytes through recognition by RIG-I and MDA5. J. Virol. 84, 6472–6482.
Liebermann, H., 1982. Reinigung und Koncentrierung animaler Viren. VEB Gustav Fischer Verlag, Jena.
Liu, Y., Cai, Y., Zhang, X., 2003. Induction of caspase-dependent apoptosis in cultured rat oligodendrocytes by murine coronavirus is mediated during cell entry and does not require virus replication. J. Virol. 77, 11952–11963.
Liu, Y., Zhang, X., 2005. Expression of cellular oncogene Bcl-xL prevents coronavirus-induced cell death and converts acute to persistent infection in progenitor rat oligodendrocytes. J. Virol. 79, 47–56.
Livak, K.J., Schmittgen, T.D., 2001. Analysis of relative gene expression data using real-time quantitative PCR and the 2(−delta delta C(T)) method. Methods 25, 402–408.
Louis, J.C., Magal, E., Muir, D., Manthorpe, M., Varon, S., 1992. CG-4, a new bipotential glial cell line from rat brain, is capable of differentiating in vitro into either mature oligodendrocytes or type-2 astrocytes. J. Neurosci. Res. 31, 193–204.
Luytjes, W., Gerritsma, H., Bos, E., Spaan, W., 1997. Characterization of two temperature-sensitive mutants of coronavirus mouse hepatitis virus strain A59 with maturation defects in the spike protein. J. Virol. 71, 949–955.
Luytjes, W., Sturman, L.S., Bredenbeek, P.J., Charite, J., van der Zeijst, B.A., Horzinek, M.C., Spaan, W.J., 1987. Primary structure of the glycoprotein E2 of coronavirus MHV-A59 and identification of the trypsin cleavage site. Virology 161, 479–487.
Maheshwari, R.K., Banerjee, D.K., Waechter, E.J., Olden, K., Friedman, R.M., 1980a. Interferon treatment inhibits glycosylation of a viral protein. Nature (London) 287, 454–456.
Maheshwari, R.K., Jay, F.T., Friedman, R.M., 1980b. Selective inhibition of glycoprotein and membrane protein of vesicular stomatitis virus from interferon-treated cells. Science 207, 540–541.
Makino, S., Taguchi, F., Hayami, M., Fujiwara, K., 1983. Characterization of small plaque mutants of mouse hepatitis virus, JHM strain. Microbiol. Immunol. 27, 445–454.
Matthews, A.E., Lavi, E., Weiss, S.R., Paterson, Y., 2002. Neither B cells nor T cells are required for CNS demyelination in mice persistently infected with MHV-A59. J. Neurovirol. 8, 257–264.
Narayanan, K., Maeda, A., Maeda, J., Makino, S., 2000. Characterization of the coronavirus M protein and nucleocapsid interaction in infected cells. J. Virol. 74, 8127–8134.
Nash, T.C., Buchmeier, M.J., 1997. Entry of mouse hepatitis virus into cells by endosomal and nonendosomal pathways. Virology 233, 1–8.
Phillips, J.J., Chua, M.M., Lavi, E., Weiss, S.R., 1999. Pathogenesis of chimeric MHV4/MHV-A59 recombinant viruses: the murine coronavirus spike protein is a major determinant of neurovirulence. J. Virol. 73, 7752–7760.
Rottier, P.J.M., Horzinek, M.C., van der Zeijst, B.A., 1981. Viral protein synthesis in mouse hepatitis virus strain A59-infected cells: effect of tunicamycin. J. Virol. 40, 350–357.

Sawicki, S.G., Lu, J.H., Holmes, K.V., 1995. Persistent infection of cultured cells with mouse hepatitis virus (MHV) results from the epigenetic expression of the MHV receptor. J. Virol. 69, 5535–5543.
Schickli, J.H., Zelus, B.D., Wentworth, D.E., Sawicki, S.G., Holmes, K.V., 1997. The murine coronavirus mouse hepatitis virus strain A59 from persistently infected murine cells exhibits an extended host range. J. Virol. 71, 9499–9507.
Snijder, E.J., Bredenbeek, P.J., Dobbe, J.C., Thiel, V., Ziebuhr, J., Poon, L.L.M., Guan, Y., Rozanow, M., Spaan, W.J.M., Gorbalenya, A.E., 2003. Unique and conserved features of genome and proteome of SARS-coronavirus, an early split-off from the coronavirus group 2 lineage. J. Mol. Biol. 331, 991–1004.
Sorensen, O., Saravani, A., Dales, S., 1987. In vivo and in vitro models of demyelinating disease. XVII. The infectious process in athymic rats inoculated with JHM virus. Microbial. pathogen. 2, 79–90.
Stauber, R., Pfleiderera, M., Siddell, S., 1993. Proteolytic cleavage of the murine coronavirus surface glycoprotein is not required for fusion activity. J. Gen. Virol. 74, 183–191.
Stohlman, S.A., Lai, M.M., 1979. Phosphoproteins of murine hepatitis viruses. J. Virol. 32, 672–675.
Suzuki, H., Taguchi, F., 1996. Analysis of the receptor-binding site of murine coronavirus spike protein. J. Virol. 70, 2632–2636.
Vennema, H., Godeke, G.J., Rossen, J.W.A., Voorhout, W.F., Horzinek, M.C., Opstelten, D.J.E., Rottier, P.J.M., 1996. Nucleocapsid-independent assembly of coronavirus-like particles by coexpression of viral envelope proteins. EMBO J. 15, 2020–2028.
Verity, A.N., Redesen, D.B., Vonderscher, C., Handley, V.W., Campagnoni, A.T., 1993. Expression of myelin protein genes and other myelin components in an oligodendrocytic cell line conditionally immortalized with a temperature-sensitive retrovirus. J. Neurochem. 60, 577–587.
Wang, F.I., Stohlman, S.A., Flemming, J.O., 1990. Demyelination induced by murine hepatitis virus JHM strain (MHV-4) is immunologically mediated. J. Neuroimmunol. 30, 31–41.
Wu, G.F., Dandekar, A.A., Pewe, L., Perlman, S., 2000. CD4 and CD8 T cells have redundant bu not identical roles in virus-induced demyelination. J. Immunol. 165, 2278–2286.
Wu, G.F., Perlman, S., 1999. Macrophage infiltration, but not apoptosis, is correlated with immune-mediated demyelination following nurine infection with a neurotropic coronavirus. J. Virol. 73, 8771–8780.
Yu, X., Bi, W., Weiss, S.R., Leibowitz, J.L., 1994. Mouse hepatitis virus gene 5b protein is a new virion envelope protein. Virology 202, 1018–1023.
Zhang, X., Herbst, W., Kousoulas, K.G., Storz, J., 1994. Biological and genetic characterization of a hemagglutinating coronavirus isolated from a diarrhoeic child. J. Med. Virol. 44, 152–161.
Zhang, X., Lai, M.M., 1994. Unusual heterogeneity of leader–mRNA fusion in a murine coronavirus: implications for the mechanism of RNA transcription and recombination. J. Virol. 68, 6626–6633.
Zhu, H., Yu, D., Zhang, X., 2009. The spike protein of murine coronavirus regulates viral genome transport from the cell surface to the endoplasmic reticulum during infection. J. Virol. 83, 10633–10653.